JOURNAL OF QUATERNARY SCIENCE (2020) **35**(6) 803–816 ISSN 0267-8179. DOI: 10.1002/jqs.3228

JQS Journal of Quaternary Science QRA Quaternary Research Association

Hekla 1947, 1845, 1510 and 1158 tephra in Finland: challenges of tracing tephra from moderate eruptions

MAARIT KALLIOKOSKI,[1,2]* ESTHER RUTH GUÐMUNDSDÓTTIR[1] and STEFAN WASTEGÅRD[3]
[1]Nordic Volcanological Centre, Institute of Earth Sciences, University of Iceland, Iceland
[2]Department of Geography and Geology, University of Turku, Finland
[3]Department of Physical Geography, Stockholm University, Sweden

Received 22 January 2020; Revised 29 May 2020; Accepted 12 June 2020

ABSTRACT: Several cryptotephra layers that originate from Icelandic volcanic eruptions with a volcanic explosivity index (VEI) of ≤ 4 and tephra volumes of < 1 km^3 have previously been identified in Northern Europe, albeit within a restricted geographical area. One of these is the Hekla 1947 tephra that formed a visible fall-out in southern Finland. We searched for the Hekla 1947 tephra from peat archives within the previously inferred fall-out zone but found no evidence of its presence. Instead, we report the first identification of Hekla 1845 and Hekla 1510 cryptotephra layers outside of Iceland, the Faroe Islands, Ireland and the UK. Additionally, Hekla 1158 tephra was found in Finland for the first time. Our results confirm that Icelandic eruptions of moderate size can form cryptotephra deposits that are extensive enough to be used in inter-regional correlations of environmental archives and carry a great potential for refining regional tephrochronological frameworks. Our results also reveal that Icelandic tephra has been dispersed into Finnish airspace at least seven times during the past millennium and in addition to a direct eastward route the ash clouds can travel either via a northerly or a southerly transport pathway.

KEYWORDS: cryptotephra; Finnish tephrochronology; Hekla 1947; Hekla volcano; Icelandic moderate eruptions

Introduction

Cryptotephra layers produced by very large (VEI ≥ 5: Newhall and Self, 1982) silicic explosive eruptions of Icelandic volcanoes form the backbone of the North European tephrochronological frameworks and provide powerful tools for dating and correlating palaeoenvironmental archives such as peat sequences and lake sediment records from the Last Glacial–Interglacial transition (LGIT) and the Holocene (e.g. Wastegård and Davies, 2009; Lawson *et al.*, 2012; Davies *et al.*, 2012; Timms *et al.*, 2019). In addition to these major marker layers, cryptotephra horizons from Icelandic smaller scale (VEI ≤ 4) eruptions (e.g. Dugmore *et al.*, 1996; Rea *et al.*, 2012; Watson *et al.*, 2015), as well as ultra-distal cryptotephra deposits that are sourced from other continents and volcanic centres, have been detected across Northern Europe (e.g. Jensen *et al.*, 2014; van der Bilt *et al.*, 2017; Plunkett and Pilcher, 2018; Jones *et al.*, 2019). Icelandic eruptions of VEI ≤ 4 have generally produced tephra isochrones with restricted dispersal areas in the distal field (Lawson *et al.*, 2012) and most of the ultra-distal cryptotephras have been identified at single sites thus far (e.g. Plunkett and Pilcher, 2018; van der Bilt and Lane, 2019). However, the potential for both ultra-distal tephra and tephra from Icelandic smaller scale eruptions to be used as regional and inter-regional isochrones may improve with new and better methods for extracting and analysing small amounts of tephra from peat and minerogenic deposits. For example, picking individual glass shards for geochemical analysis using a micromanipulator (Lane *et al.*, 2014; MacLeod *et al.*, 2014) and optimising the electron microprobe analysis protocols for geochemical fingerprinting of single glass grains as small as 10 µm (Hayward, 2012) enable source eruptions of cryptotephra deposits consisting of very scarce and small shards to be traced.

So far, the majority of the historical (younger than 870 AD) tephras originating from Icelandic smaller scale eruptions remain undetected in distal areas. However, a simulation of transport, dispersion and deposition of volcanic ash from an explosive Hekla eruption based on an atmospheric circulation model demonstrated that an initial plume height of just 12 km would give a > 45% probability of ash fall-out in Scotland and Fennoscandia (Leadbetter and Hort, 2011). As all the 18 historical Hekla eruptions have started with an explosive phase during which a sustained tephra plume has reached a height of 12–36 km (Thorarinsson, 1967; Janebo *et al.*, 2016), each of these eruptions, independent of size, carries the potential to form distally transported cryptotephra deposits in the North European palaeoenvironmental records.

The scarcity of cryptotephra deposits from historical Hekla eruptions could partly be explained by the fact that most of the tephrochronological work that uses the recently developed methods of concentrating scarce shards has focused on LGIT tephras (e.g. Larsen and Noe-Nygaard, 2013; MacLeod *et al.*, 2014; Jones *et al.*, 2018). However, the occurrence of diffuse cryptotephra layers or deposits with insufficient shard concentration for geochemical analysis is relatively common at shallow depths in peat stratigraphies (e.g. Boygle, 2004; Wastegård *et al.*, 2008; Housley *et al.*, 2010; Watson *et al.*, 2015) and could indicate the presence of tephra from several historical Icelandic eruptions. Geochemically identified cryptotephra horizons produced by eruptions of VEI ≤ 4 include three separate historical Hekla layers that are present in Ireland and the UK; namely, Hekla 1510 (Dugmore *et al.*, 1996; Pilcher *et al.*, 1996; Reilly and Mitchell, 2015), Hekla 1845 (Watson *et al.*, 2015, 2017) and Hekla 1947 (Rea *et al.*, 2012; Watson *et al.*, 2015). Each of these layers has been used as a local or regional correlation and

*Correspondence: Maarit Kalliokoski, as above.
E-mail: mhk1@hi.is; mkalli@utu.fi

dating horizon in environmental research in the UK and Ireland (Hall, 1998; Housley *et al.*, 2010; Watson *et al.*, 2015), but it is not yet well established whether these smaller scale tephras could form isochrones that are extensive enough to allow for inter-regional correlations in the distal area. Until now, no distal deposits from the Hekla 1947, 1845 or 1510 eruptions have been identified with certainty further afield outside of Ireland and the UK, even if contemporary eyewitness accounts reveal that the Hekla 1845 and 1947 tephras formed visible fall-out in the Shetland Islands and Finland, respectively (Salmi 1948; Thorarinsson, 1981). Additionally, a cryptotephra layer in the Faroe Islands has been tentatively correlated with the Hekla 1845 eruption (Wastegård, 2002), and a diffuse deposit consisting of very scarce shards that possibly originate from historical eruption (s) of Hekla was recently reported from northwestern Russia (Vakhrameeva *et al.*, 2020).

In this paper we discuss several attempts at finding the Hekla 1947 tephra as well as other Icelandic historical tephras from 25 Finnish peatlands. We report the first identification of the Hekla 1845, Hekla 1510 and Hekla 1158 cryptotephra deposits in southern and central Finland, thus extending their known dispersal areas significantly further east. We also present new results on the geochemical composition of Hekla 1845 tephra from a proximal site in Iceland as well as new data on the physical properties and geochemical composition of the Hekla 1947 tephra sample collection (Salmi, 1948). Finally, we discuss preservation issues of scarce cryptotephra deposits in environmental archives and the potential for smaller scale eruptions to form widespread isochrones in the far-distal field.

Research area and methods

Site selection and sampling

Our main research area comprises 18 peatlands (Table 1, Fig. 1) that are within the fall-out zone of the Hekla 1947 tephra in southern Finland as inferred by Salmi (1948). Additionally, four peatland sites outside of the fall-out zone (7, 15, 18 and 20 in Fig. 1) and three sites in west-central Finland, in the proximity of an unconfirmed eyewitness report of tephra fall-out (Salmi 1948) were chosen for investigation (10–12 in Fig. 1). A previous search for Hekla 1947 tephra at bog and lake sites in Finland failed to detect any shards within the fall-out zone (Kalliokoski *et al.*, 2019), which could indicate either a highly patchy tephra fall-out within the dispersal area, a sporadic occurrence of the tephra in environmental archives due to post-depositional processes, or preservation issues (Boygle, 1999; Bergman *et al.*, 2004; Payne and Gehrels, 2010; Watson *et al.*, 2015). Given that a possible connection between precipitation and the amount of tephra fall-out has been suggested in earlier studies (Dugmore *et al.*, 1995; Langdon and Barber, 2004; Rea *et al.*, 2012), precipitation maps for the days following the 29 March 1947 Hekla eruption were generated from the Finnish Meteorological Office weather data (Fig. 2A–C) and used as an aid for site selection. Sites with both high and low precipitation were selected (Fig. 1 and 2A–C) to test for a correlation between shard concentration and precipitation amount. Additionally, a snow-depth map for 30 March 1947 was prepared from the Finnish Meteorological Office data (Fig. 2D) to search for potentially snow-free peatlands where spring melt would not have redistributed the tephra deposits (Boygle, 1999; Bergman *et al.*, 2004). Peatlands within a 20 km radius of the nearest weather station were targeted to ensure the validity of weather data at our research sites (Fig. 1). To minimise the likelihood of post-depositional disturbance of tephra layers by anthropogenic activity, peatlands in nature conservation areas were prioritised. Therefore, protected blanket mires were preferred over drained or cut ombrotrophic peat bogs, even if it has been suggested that raised peat bogs better record and preserve primary atmospheric fall-out of tephra (e.g. Persson, 1966; Bergman *et al.*, 2004; Gehrels *et al.*, 2008).

Peat samples were collected from each peatland site during the summer field seasons of 2014 and 2015 using a Russian

Table 1. Coordinates of investigated peatland sites.

No.	Research site (code)	Monolith length (cm)	Length of investigated core (cm)	Protection status	Lat. (N)	Long. (E)
1	Stormossen (STOR)	36, 20, 28, 20, 25	90	Not protected	60.12	19.75
2	Kolkansuo (KOL)	–	90	Protected	60.82	22.11
3	Kaukosuo (KAU)	26	90	Protected	60.83	22.23
4	Rehtsuo (REHT)	35	90	Protected	60.60	22.25
5	Kurjenrahka (KUR)	34, 33, 36	-	Protected	60.72	22.40
6	Kontolanrahka (KON)	–	90	Protected	60.77	22.78
7	Suovanalanen (SUO)	27	90	Not protected	61.92	23.50
8	Torronsuo (TOR)	–	50	Protected	60.72	23.61
9	Purinsuo (PUR)	–	50	Not protected. Drained	60.71	24.03
10	Kivihypönneva (KIVI)	23	90	Not protected. Drained	63.50	24.12
11	Pakosuo (PAKO)	50	-	Protected	63.27	24.69
12	Pervarvikonneva (PER)	33, 34	90	Protected	63.26	24.87
13	Isosuo (ISO)	21	50	Not protected	60.66	25.23
14	Haapasuo (HAA)	24	90	Protected	61.91	26.05
15	Kananiemensuo (KANA)	23	90	Protected	60.57	26.71
16	Hangassuo (HANG)	20	50	Not protected	60.79	26.91
17	Tarilampi (TAR)	22	50	Not protected	61.74	27.22
18	Hallinsuo (HAL)	21	50	Protected. Drained	60.58	27.64
19	Vuotsinsuo (VUOT)	23	50	Protected. Drained	62.10	27.88
20	Hämmäauteensuo (HÄM)	27.5	50	Protected	61.01	28.29
21	Punkaharju (PUN)	30	90	Protected	61.79	29.31
22	Kyhönsuo (KYHÖ)	–	50	Not protected	62.52	30.91
23	Parkusuo (PAR)	–	50	Not protected. Drained	62.42	30.99
24	Koivusuo (KOI)	–	50	Protected	62.99	31.35
25	Hanhisuo (HAN)	–	90	Protected	62.89	31.51

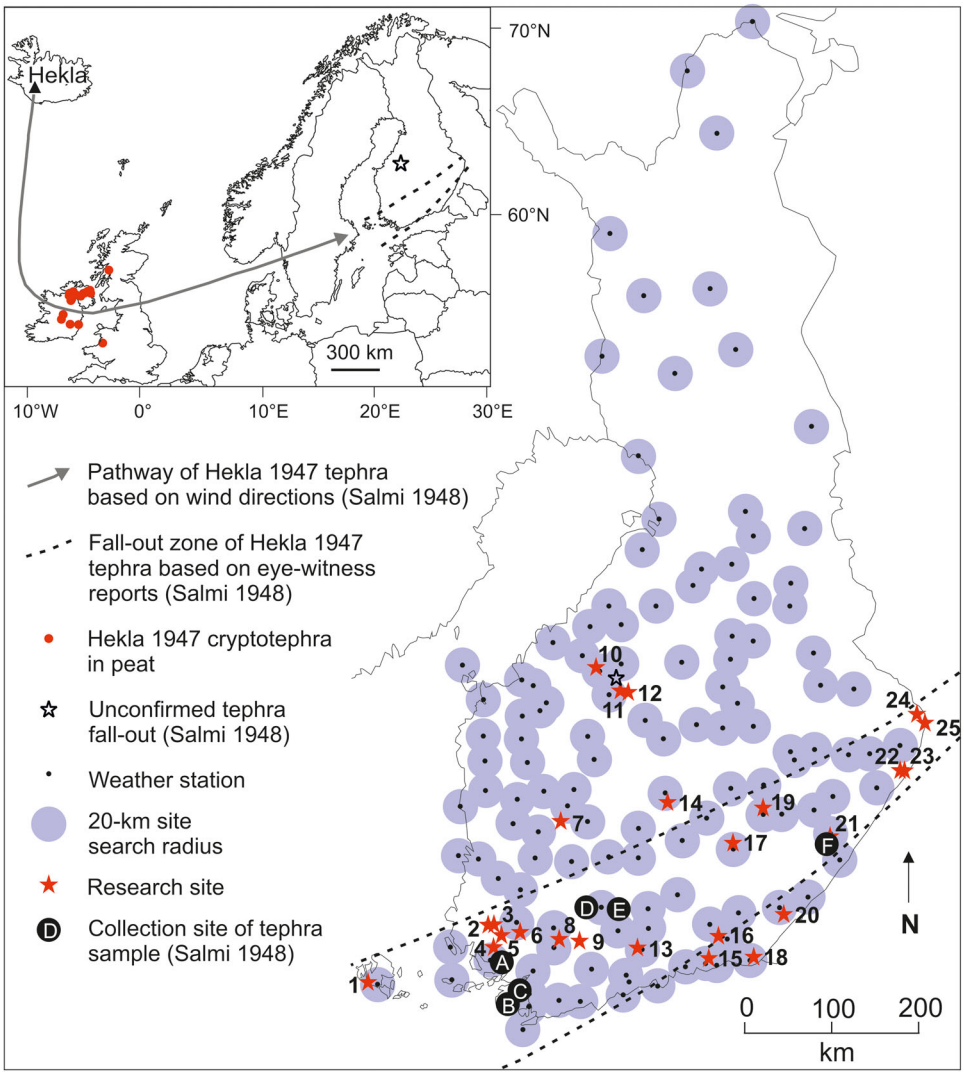

Figure 1. Locations of weather stations, investigated peatland sites (1–25) and collection sites of Hekla 1947 tephra (A–F). 1. Stormossen, 2. Kolkansuo, 3. Kaukosuo, 4. Rehtsuo, 5. Kurjenrahka, 6. Kontolanrahka, 7. Suovanalanen, 8. Torronsuo, 9. Purinsuo, 10. Kivihypönneva, 11. Pakosuo, 12. Pervarvikonneva, 13. Isosuo, 14. Haapasuo, 15. Kananiemensuo, 16. Hangassuo, 17. Tarilampi, 18. Hallinsuo, 19. Vuotsinsuo, 20. Hämmäauteensuo, 21. Punkaharju, 22. Kyhönsuo, 23. Parkusuo, 24. Koivusuo, 25. Hanhisuo. A = Västanfjärd, B = Viksvidja, C = Littoinen, D = Kuusjoki, E = Tuulos, F = Punkaharju. The transport pathway and the fall-out zone of Hekla 1947 are from Salmi (1948). Occurrence of Hekla 1947 cryptotephra in Ireland and the UK is from Housley *et al.* (2010); Rea *et al.* (2012) and Watson *et al.* (2017). [Color figure can be viewed at wileyonlinelibrary.com]

peat corer with a 50 cm long and 5 cm wide cylinder. Successive samples with a 10 cm overlap were cored from the full peat stratigraphy. An additional 20–50 cm long monolith with a cross section of 10×10 cm was cut from the uppermost peat of 14 sites using a sharp knife and multiple monoliths were collected from three sites (Table 1). The cores were wrapped in plastic and stored in cool conditions until subsampling.

A proximal sample of Hekla 1845 tephra was collected from a soil section (64.04 N°, 19.32 W°) in Iceland in 2018 for improving the proximal geochemistry dataset. This tephra was identified in the field based on its physical properties (colour and grain size) as well as its stratigraphic position below the Katla 1918 tephra marker layer. A sample covering the full thickness (1 cm) of the tephra layer was collected into a plastic bag and stored refrigerated until laboratory processing.

Additionally, the Hekla 1947 tephra sample collection of Salmi (1948) was reinvestigated in 2016. This collection consists of six tephra samples that had been recovered from snow cover and various other surfaces shortly after the fall-out and stored in sealed glass vials ever since (Salmi 1948). The collection sites of these samples are shown in Fig. 1.

Tephra extraction and processing

A subsample of one of the bottled Hekla 1947 samples (Västanfjärd) was treated with heavy liquid to determine the density range of the tephra shards. Sodium polytungstate solutions with densities of 2.2–2.7 g/cm^3 in 0.1 g/cm^3 steps were prepared and tephra shards retained in each density fraction (from < 2.2 g/cm^3 to > 2.7 g/cm^3) were mounted on glass slides with Canada Balsam and counted under a polarising microscope. Shards were also photographed for documentation, and their longest axis was measured to ascertain the average particle size of the tephra. All six samples in the collection were cleaned by floating off impurities using heavy liquid with a density of 2.2 g/cm^3 and subsequently mounted in epoxy resin for electron probe microanalysis (EPMA).

The proximal sample of Hekla 1845 tephra was cleaned by sieving with 120 and 63 µm meshes and the fraction remaining on the 63 µm sieve was mounted in an epoxy stub for EPMA.

The extraction of tephra from the Finnish peat bogs was performed in two steps. First, the uppermost 50–90 cm of the peat stratigraphy at each site was investigated for the presence

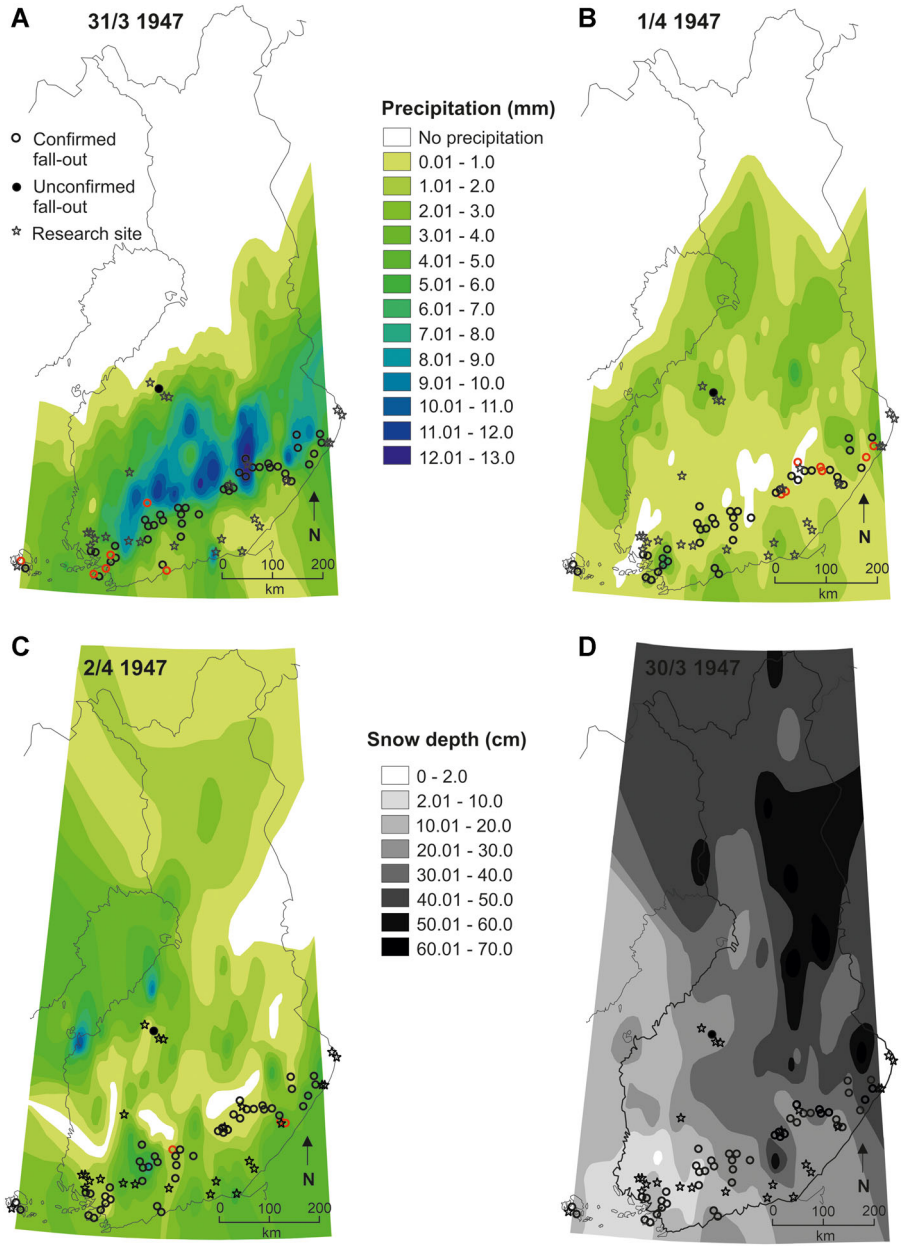

Figure 2. (A–C) Precipitation maps for the days following the 29 March 1947 eruption of Hekla. Sites for eyewitness reports on tephra fall-out are from Salmi (1948). Locations where tephra fall-out was confirmed to have occurred on each day are highlighted with red circles. Precipitation values are interpolated from weather station data of the Finnish Meteorological Institute using inverse distance weighing of the five closest data points. (D) Snow depth map for 30 March 1947. [Color figure can be viewed at wileyonlinelibrary.com]

of glass shards. The peat monoliths were initially cut into 3–5 cm-long contiguous subsamples, whereas the peat cores were subsampled in 10 cm increments. Where tephra shards were identified, new 1 cm-thick contiguous subsamples of 4 cm^3 were prepared. The samples were dried overnight at 105 °C, combusted at 550 °C for two hours and treated with 10% HCl for five hours. Sieving was avoided to ensure that even the smallest grains of volcanic glass were captured, as most of the Hekla 1947 tephra shards in Finland had been reported to measure just ca. 3 μm and only occasionally exceed 15 μm (Salmi, 1948). Instead, sodium polytungstate heavy liquid was used to clean the samples and extract the 2.3–2.5 g/cm^3 density fraction (Turney, 1998). The samples were then mounted on microscope slides using Canada Balsam, and tephra shards were counted under a polarising microscope to determine the depth of peak shard concentration.

The second step included a refined investigation of the peat samples based on the examination of the Hekla 1947 tephra collection of Salmi (1948). New 3 cm-long contiguous subsamples were extracted from each peat monolith and examined using laboratory methods that were adjusted to the results gained from the investigation of the Hekla 1947 tephra collection (see Results section). Sample volume was increased to ca. 10 cm^3 of fresh peat for every centimetre of the sampled depth range to increase the chances of finding even scarce shards. Samples were additionally sieved with a 25 μm mesh and heavy liquid densities were adjusted to extract the 2.3–2.6 g/cm^3 fraction.

Samples for EPMA were chosen from the depth of peak shard concentrations in the peat cores and treated with acid digestion instead of combustion to avoid geochemical alteration of volcanic glass at high temperatures (Pilcher and Hall, 1992; Dugmore *et al.*, 1995). Tephra shards were then handpicked using a micromanipulator and mounted in epoxy resin.

EPMA

Major element composition of 6–27 tephra shards in each sample was determined by wavelength dispersive spectrometry on either JEOL JXA-8230 SuperProbe at the Institute of Earth Science (IES), University of Iceland or Cameca SX100 at the Tephra Analysis Unit (TAU) of the University of Edinburgh. Two samples (Punkaharju and KAN90) were analysed at both IES and TAU to confirm that the two instruments produce

comparable results (Table S1). Information on the respective electron microprobes and their configuration as well as analysis settings is available in supporting material (Table S1) and in Hayward (2012).

Radiocarbon dating

The Kivihypönneva site was selected for radiocarbon dating due to its high number of cryptotephra horizons. Moss (*Sphagnum* sp.) stems and leaves were picked for radiocarbon dating from the peat at 80–81 cm depth to determine a maximum age for the investigated sequence. Radiocarbon dating was performed at the Aarhus AMS Centre. The obtained radiocarbon age was calibrated using the online version of OxCal 4.3 (Bronk Ramsey, 2009) with the IntCal-13 calibration curve (Reimer *et al.*, 2013).

Results

Hekla 1947 tephra collected by Salmi (1948)

The Hekla 1947 tephra in Finland consists of colourless to brown shards with an average grain size of around 80 µm (Fig. 3A), much larger than previously reported (Salmi, 1948). The density range of the glass grains is 2.2–2.7 g/cm^3 while the majority of them fall within the density range of 2.5–2.6 g/cm^3 (Fig. 3B). Colourless shards are present only in the 2.2–2.4 g/cm^3 density fraction, whereas brown shards exhibit a full range of densities (Fig. 4A–D). The colour of each analysed shard in two samples (Punkaharju and Kuusjoki) was recorded during the EPMA sessions, but no correlation was found between the chemical composition and the shard colour (Table S1). In the Finnish samples, the SiO_2 content of the tephra ranges from 60 to 64.5 wt%, consistent with results from the proximal area (Tables 2 and S1). However, glass grains with $SiO_2 > 69$ wt% that have been recorded at proximal sites (Larsen *et al.*, 1999), are seemingly absent from the Finnish samples.

Proximal sample of Hekla 1845 tephra

We analysed 15 shards of proximal Hekla 1845 tephra with an electron microprobe. The majority of the shards are of andesitic composition with an SiO_2 content of 57–62 wt%, whereas three shards are basaltic, and one shard is rhyolitic (Table S1). Tephra deposits from Hekla are known to have a range in chemical composition from basaltic to rhyolitic (Sigvaldason, 1974; Larsen and Thorarinsson, 1977; Guðmundsdóttir *et al.*, 2011a; Jónsson *et al.*, 2020).

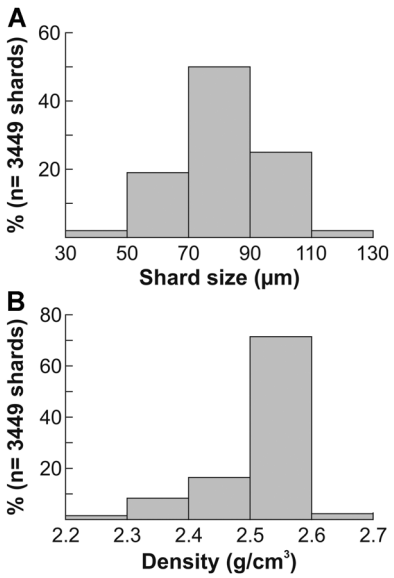

Figure 3. (A) Grain size distribution and (B) density range of the Hekla 1947 tephra shards in the Salmi (1948) sample collection from southern Finland.

Cryptotephra from peatland sites in Finland

Cryptotephra was identified in nine of our 25 research sites where it forms 19 stratigraphically discrete deposits that are composed of homogeneous tephra populations (Fig. 5 and Tables 2 and S1). The stratigraphy as well as the tephra shard concentrations of the deposits are shown in Fig. 5. The highest number of cryptotephra horizons was found in Kivihypönneva, where four separate layers were detected at the depths of 34, 52, 58 and 67 cm (Fig. 5 and Tables 2 and S1). Two sites, Pervarvikonneva and Kananiemensuo, contain three cryptotephra deposits each, at depths of 25, 60 and 65 cm and 40, 45 and 90 cm, respectively. Two cryptotephra deposits are present at three of the sites, Stormossen (at 24 and 58 cm depth), Rehtsuo (at 32 and 55 cm depth) and Suovanalanen (at 51 and 83 cm depth). At Haapasuo, Tarilampi and Hanhisuo, just one cryptotephra layer was detected at 57, 29 and 60 cm depths, respectively.

We were able to geochemically characterise 12 out of the 19 detected cryptotephra deposits and confirm the presence of four separate cryptotephra layers of Icelandic origin at our sites (Tables 2 and S1). The youngest geochemically identified cryptotephra forms a horizon of colourless rhyolitic glass with shard concentrations ranging from 15 to > 500 shards/cm^3 at six sites at depths of 29–60 cm (Fig. 5). This layer was found for the first time at two of these sites, Kivihypönneva and Kananiemensuo, whereas the occurrence and geochemical composition of this cryptotephra in Rehtsuo, Haapasuo, Tarilampi and Hanhisuo has already been published (Kalliokoski *et al.*, 2019). EPMA of 17 individual shards indicates an Icelandic provenance for this tephra and plotting the results on a total alkali–silica (TAS) diagram reveals that the glass composition matches the geochemical envelope of the proximal products of the Askja volcano (Table 2 and Fig. 6A).

The second youngest geochemically identified cryptotephra horizon is present at just one site, Kananiemensuo, where it is positioned at the depth of 45 cm, approximately 5 cm below the Askja horizon (Fig. 5). This deposit consists of a small amount (<50 shards/cm^3) of light brown to dark brown tephra shards (Fig. 4E–F). Major element characterisation of eight shards from this layer shows a geochemical affinity with the andesitic proximal products of the Hekla volcano when the results are plotted on a TAS diagram (Fig. 6A and Table 2).

The second oldest geochemically characterised cryptotephra layer occurs in Kivihypönneva at 58 cm depth, in Pervarvikonneva at 60 cm depth and in Kananiemensuo at 90 cm depth. The peak shard concentration range for this layer is 60–80 shards/cm^3 and the shards are light brown with varying morphologies (Fig. 4G–H). EPMA results were obtained from 7–19 individual glass grains per layer and they plot within the geochemical envelope of andesitic–dacitic Hekla products on the TAS diagram (Tables 2 and S1, Fig. 6A).

The oldest geochemically fingerprinted cryptotephra layer is present at two sites: in Kivihypönneva at 67 cm depth and in Pervarvikonneva at 65 cm depth. It comprises a mixture of brown and colourless thin glass grains with fluted and vesicular morphologies (Figs 5 and 4I–J). Peak shard concentrations of this layer are 52 shards/cm^3 in Pervarvikonneva and 98 shards/cm^3 in Kivihypönneva. Despite the relatively high shard concentrations, EPMA succeeded for just 6 and 10 glass grains in Pervarvikonneva and Kivihypönneva, respectively,

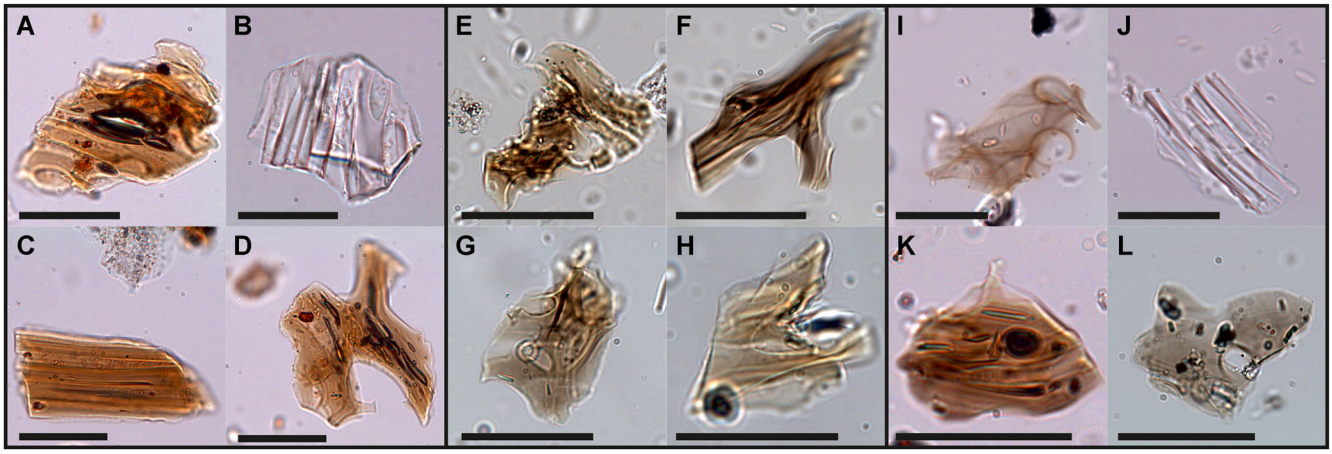

Figure 4. Cryptotephra shards detected at Finnish sites. (A–B) 2.3–2.5 g/cm^3 fraction of the Hekla 1947 tephra, (C–D) > 2.5 g/cm^3 fraction of the Hekla 1947 tephra, (E–F) Hekla 1845 tephra, (G–H) Hekla 1510 tephra, (I–J) Hekla 1158 tephra, (K–L) unidentified tephra in Pervarvikonneva and Kivihypönneva. Scale bar length in all the images is 40 µm. [Color figure can be viewed at wileyonlinelibrary.com]

due to very thin shard walls (Table 2). Inspection of the results on a TAS diagram shows that this layer represents dacitic products of the Hekla volcano (Fig. 6A).

Geochemical characterisation of seven other cryptotephra deposits at our sites failed, either due to a lack of material for the EPMA sample preparation procedure or loss of the scarce and tiny shards during the final steps of sanding and polishing the EPMA mounts. Based on the stratigraphic position of these deposits and characteristics of the tephra shards (Fig. 5), it is likely that they originate from the same Icelandic volcanoes as the geochemically identified layers in this study. However, geochemical fingerprinting is necessary for assigning them to specific eruptions.

Radiocarbon dating

Radiocarbon dating of a peat sample (lab. ID AAR-30738) from 80 to 81 cm depth at Kivihypönneva, ca. 13 cm below the oldest cryptotephra layer, gives a ^{14}C BP age of 1947 ± 24 and a calibrated age of 1–125 AD (2σ) for that depth (Fig. 5). This indicates that all the four identified cryptotephra layers in this study were deposited during the past two millennia.

Discussion

Hekla 1947 tephra samples

The major element data of the Hekla 1947 tephra consist of 115 electron microprobe point-analyses of single shards (Table S1) and comprise a robust dataset for comparisons of future cryptotephra findings in the distal area. The analysed shards have not been subjected to possible geochemical alteration in an acidic environment, neither during preservation within the peat/sediment matrix (Pollard *et al.*, 2003) nor in laboratory procedures (Blockley *et al.*, 2005; Cooper *et al.*, 2019a). They therefore represent pristine volcanic glass of the Hekla 1947 eruption and provide a reference point for assessing the degree of geochemical alteration in tephra shards that are sourced from the same eruption and retrieved from environmental records.

The Hekla 1947 eruption (VEI 4) produced 0.18 km^3 of tephra in total (Thorarinsson, 1954). The explosive phase lasted for about 8 h and produced grey brownish tephra with SiO_2 values of 61–64 wt% during the Plinian opening stage (Thorarinsson, 1954; Thorsteinsdóttir *et al.*, 2015). The tephra erupted in later stages was of a darker colour and contained 56–58 wt% of SiO_2. The shards that were dispersed to Finland represent the Plinian phase based on their SiO_2 content of 60–64.5 wt%. The TiO_2 content of the Hekla 1947 tephra in Finland is constant at around 0.90 wt% (Fig. 7). Geochemical results from Iceland and Ireland show more scatter on bivariate plots, possibly indicating that the full range of eruption products was analysed there. When the Finnish results are compared with results from Iceland, Ireland and Britain, the highest compatibility is found between the glass compositions from Finland and Northern Ireland (Fig. 7).

Cryptotephra deposits in the Finnish peatlands

Geochemistry of the cryptotephra layers at Finnish sites was compared with the composition of proximal products of all the known Hekla and Askja eruptions of the past two millennia to determine their source eruptions (for a complete eruption list see Thorarinsson, 1967; Larsen *et al.*, 1999, 2020). For the sake of clarity, only the proximal tephras with compositions that most closely resemble the geochemistry of the Finnish deposits are shown in the bivariate plots of major element ratios to highlight the similarities and differences between these (Fig. 6B–C).

Askja 1875 AD

The uppermost geochemically fingerprinted cryptotephra layer at our sites consists of rhyolitic glass originating from the Askja 1875 eruption based on its composition (Fig. 6A–C, Table S1). The diagnostic feature of the Askja 1875 tephra is its high TiO_2 content of 0.7–1.0 wt% (Table S1), given that no other rhyolitic Icelandic tephras with TiO_2 > 0.7 wt% are known from the historical period (e.g. Larsen *et al.*, 1999). Furthermore, the 1875 eruption is the only recorded historical Askja event that produced silicic tephra, and the common presence of this tephra in Norway, Sweden and Finland (Wastegård, 2005; Davies *et al.*, 2007; Carey *et al.*, 2010; Kalliokoski *et al.*, 2019) supports the correlation made here.

Hekla 1845 AD

A cryptotephra layer in Kananiemensuo at the depth of 45 cm is correlated to the 1845 eruption of Hekla based on both its geochemistry and its stratigraphic position < 5 cm below the Askja 1875 tephra (Fig. 5). Comparison with the new proximal data of the Hekla 1845 tephra reveals a strong similarity between the deposits in Finland, Northern Ireland (Watson *et al.*, 2015) and Iceland (Table 2 and Fig. 6B–C). In Finland this tephra is andesitic with an SiO_2 content of 60–62 wt%, while at the

Table 2. Non-normalised mean major element values for Hekla 1947 tephra samples, Hekla 1845 proximal sample and cryptotephra deposits investigated in this study. Average composition of Hekla 1947, 1510 and 1158 tephras from proximal sites and Hekla 1845 from a distal site is given for reference. The number of analysed shards for each site is shown in parentheses. SD refers to one standard deviation. IES and TAU are abbreviations of the EPMA facilities. KIVI = Kivihypönneva, PER = Pervarvikonneva, KANA = Kananiemensuo.

Site/Sample code		SiO_2	TiO_2	Al_2O_3	FeO	MnO	MgO	CaO	Na_2O	K_2O	P_2O_5	Total
KIVI 52												
Askja 1875 (10)	*Mean*	*72.49*	*0.83*	*12.67*	*3.49*	*0.12*	*0.72*	*2.48*	*3.71*	*2.36*	*0.15*	*99.01*
IES	SD	1.24	0.07	0.24	0.30	0.03	0.07	0.22	0.56	0.08	0.03	1.01
KIVI 58												
Hekla 1510 (7)	*Mean*	*61.72*	*0.91*	*15.32*	*7.69*	*0.23*	*1.26*	*4.38*	*4.40*	*1.70*	*0.31*	*97.93*
IES	SD	0.91	0.05	0.28	0.20	0.03	0.08	0.10	0.20	0.09	0.05	1.15
KIVI 67												
Hekla 1158 (10)	*Mean*	*66.57*	*0.48*	*14.62*	*5.53*	*0.17*	*0.44*	*3.03*	*4.68*	*2.26*	*0.09*	*97.88*
IES	SD	1.99	0.03	0.50	0.16	0.02	0.06	0.20	0.43	0.11	0.03	2.42
PER 60												
Hekla 1510 (19)	*Mean*	*61.68*	*0.92*	*15.29*	*7.51*	*0.21*	*1.33*	*4.48*	*4.44*	*1.66*	*0.31*	*97.83*
IES	SD	0.94	0.05	0.24	0.37	0.04	0.09	0.18	0.30	0.09	0.04	1.31
PER 65												
Hekla 1158 (5)	*Mean*	*67.45*	*0.46*	*14.70*	*5.53*	*0.18*	*0.45*	*3.01*	*4.38*	*2.31*	*0.09*	*98.56*
IES	SD	0.35	0.01	0.23	0.24	0.01	0.01	0.09	0.32	0.05	0.03	0.60
KANA 40												
Askja 1875 (7)	*Mean*	*72.47*	*0.83*	*12.52*	*3.60*	*0.11*	*0.74*	*2.55*	*4.10*	*2.42*	*0.15*	*99.48*
TAU	SD	1.16	0.09	0.47	0.39	0.01	0.15	0.28	0.21	0.11	0.04	1.01
KANA 45												
Hekla 1845 (8)	*Mean*	*60.90*	*1.10*	*15.73*	*8.80*	*0.24*	*1.52*	*5.00*	*4.61*	*1.55*	*0.38*	*99.85*
TAU	SD	0.78	0.05	0.32	0.45	0.01	0.08	0.19	0.14	0.08	0.03	0.59
KANA 90												
Hekla 1510 (8)	*Mean*	*61.04*	*0.90*	*15.04*	*7.58*	*0.23*	*1.22*	*4.43*	*4.50*	*1.76*	*0.29*	*97.00*
TAU + IES	SD	0.89	0.04	0.53	0.18	0.03	0.03	0.14	0.28	0.11	0.05	1.46
Hekla 1947												
Västanfjärd (19)	*Mean*	*61.72*	*0.90*	*15.33*	*7.65*	*0.22*	*1.18*	*4.43*	*4.58*	*1.80*	*0.27*	*98.09*
TAU	SD	0.67	0.03	0.52	0.28	0.01	0.06	0.19	0.38	0.08	0.01	1.43
Viksvidja (17)	*Mean*	*62.69*	*0.90*	*13.94*	*7.86*	*0.22*	*1.21*	*4.48*	*4.46*	*1.81*	*0.22*	*97.80*
TAU	SD	0.79	0.02	0.63	0.45	0.01	0.07	0.21	0.35	0.12	0.01	1.14
Littoinen (15)	*Mean*	*62.73*	*0.86*	*15.40*	*7.73*	*0.21*	*1.20*	*4.42*	*4.47*	*1.73*	*0.27*	*99.02*
TAU	SD	0.75	0.04	0.46	0.30	0.02	0.07	0.21	0.40	0.08	0.02	1.55
Kuusjoki (21)	*Mean*	*61.82*	*0.89*	*14.35*	*8.04*	*0.22*	*1.23*	*4.56*	*4.53*	*1.73*	*0.26*	*97.63*
TAU	SD	0.76	0.03	0.41	0.43	0.01	0.05	0.17	0.32	0.06	0.02	1.05
Tuulos (11)	*Mean*	*62.27*	*0.89*	*15.33*	*8.05*	*0.23*	*1.27*	*4.52*	*4.63*	*1.74*	*0.26*	*99.19*
TAU	SD	0.45	0.02	0.38	0.31	0.01	0.07	0.16	0.21	0.10	0.01	0.76
Punkaharju (27)	*Mean*	*62.74*	*0.89*	*14.71*	*7.90*	*0.22*	*1.23*	*4.52*	*4.61*	*1.70*	*0.25*	*98.77*
TAU + IES	SD	0.54	0.06	0.53	0.42	0.02	0.07	0.17	0.22	0.10	0.03	0.94
Iceland (10)	*Mean*	*62.15*	*0.98*	*15.13*	*8.01*	*0.22*	*1.28*	*4.46*	*4.38*	*1.73*	–	*98.40*
Larsen *et al.*, 1999	SD	1.49	0.14	0.12	0.44	0.02	0.21	0.31	0.55	0.08	–	0.96
Hekla 1845												
Iceland (11)	*Mean*	*60.47*	*1.28*	*15.26*	*9.03*	*0.26*	*1.74*	*5.12*	*4.29*	*1.62*	*0.50*	*99.57*
IES	SD	2.08	0.16	0.44	1.04	0.04	0.35	0.69	0.32	0.32	0.14	0.80
N Ireland (15)	*Mean*	*60.74*	*1.07*	*14.87*	*8.59*	*0.23*	*1.57*	*4.97*	*4.28*	*1.66*	*0.42*	*98.38*
Watson *et al.*, 2015	SD	0.99	0.09	0.24	0.47	0.02	0.18	0.24	0.19	0.10	0.05	1.00
Faroe Islands (10)	*Mean*	*61.30*	*0.92*	*15.02*	*8.34*	*0.30*	*1.44*	*4.73*	*4.41*	*1.54*	–	*97.98*
Wastegård, 2002	SD	2.22	0.26	0.43	1.02	0.10	0.59	0.68	0.31	0.23	–	–
Hekla 1510												
Iceland (10)	*Mean*	*62.65*	*0.96*	*15.22*	*7.80*	*0.23*	*1.30*	*4.50*	*4.42*	*1.75*	–	*98.82*
Larsen *et al.*, 1999	SD	0.61	0.08	0.17	0.16	0.03	0.08	0.17	0.24	0.04	–	0.88
Hekla 1158												
Iceland (7)	*Mean*	*67.42*	*0.48*	*14.39*	*5.71*	*0.20*	*0.45*	*3.11*	*4.56*	*2.24*	–	*98.55*
Larsen *et al.*, 1999	SD	0.58	0.06	0.21	0.08	0.02	0.04	0.14	0.28	0.07	–	1.01

proximal site in Iceland basaltic glass and one rhyolitic shard were also analysed (Table S1), and in Northern Ireland a minor rhyolitic component has been identified alongside the predominant andesitic component (Watson *et al.*, 2015). The Hekla 1845 tephra can be clearly distinguished from other known historical products of Hekla by its FeO/K_2O ratio (Fig. 6B).

Hekla 1510 AD

Andesitic–dacitic cryptotephra of Hekla origin was identified at our southernmost site in Kananiemensuo as well as in west-central Finland in Kivihypönneva and Pervarvikonneva. Both the geochemical composition and stratigraphic position of this layer below the Askja 1875 and Hekla 1845 deposits support a correlation to the Hekla 1510 eruption (Fig. 5 and Tables 2 and S1). The geochemical compositions of the Hekla 1947 and Hekla 1510 tephras are almost identical based on the proximal data (Larsen *et al.*, 1999), but the stratigraphic position of this layer at Finnish sites below the Askja 1875 cryptotephra horizon excludes the 1947 eruption as its source. The lower FeO content (< 8 wt%) of the Hekla 1510 tephra distinguishes it from historical andesitic Hekla products

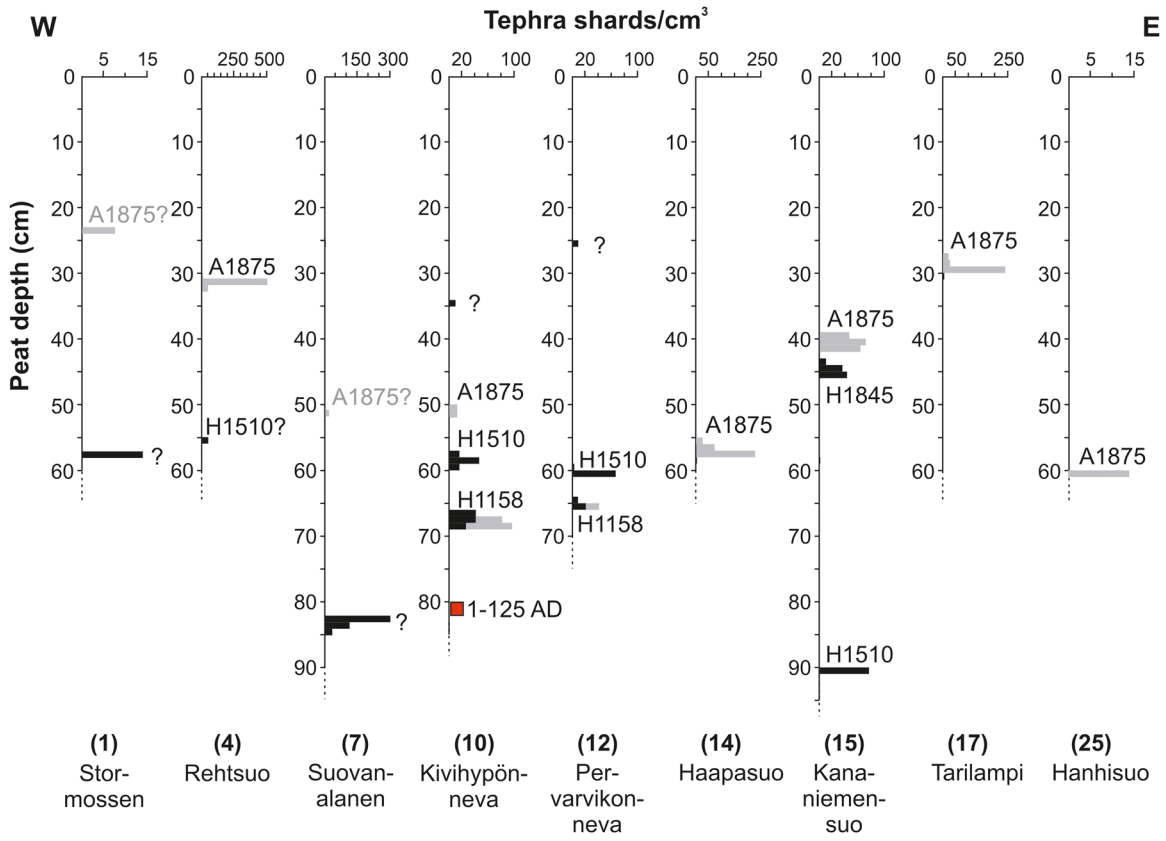

Figure 5. Tephra shard concentration profiles for the peatland sites in this study. Deposits consisting of colourless shards are marked in grey and brownish shards in black. The red square marks the position of the radiocarbon-dated peat sample. Unidentified layers are labelled with a question mark. [Color figure can be viewed at wileyonlinelibrary.com]

(H1845, H1636 and H1300) as is clearly demonstrated in the FeO/TiO_2 and FeO/K_2O bivariate plots (Fig. 6B–C).

Hekla 1158 AD

The oldest identified cryptotephra layer at our sites is the dacitic Hekla 1158 layer in Kivihypönneva and Pervarvikonneva, where it is positioned <10 cm below the Hekla 1510 cryptotephra horizon. The Hekla 1158 tephra can be distinguished from the other historical silicic Hekla tephra, the Hekla 1104, based on its significantly lower (66.4–68.2 wt%) SiO_2 and higher FeO content (Fig. 6B–C; Larsen *et al.*, 1999). Correlation of this cryptotephra layer in Finland to the Hekla 1158 eruption is also supported by its earlier identification in northern parts of Norway and Sweden (Pilcher *et al.*, 2005; Balascio *et al.*, 2011; Watson *et al.*, 2016; Cooper *et al.*, 2019b).

Absence of the Hekla 1947 tephra from Finnish sites

We searched for the Hekla 1947 tephra by a thorough and repeated investigation of peat samples. We modified the routine laboratory methods based on investigation of Hekla 1947 shard properties but failed to locate any tephra shards that could be confidently assigned to the 1947 eruption. At two sites in west-central Finland, in the vicinity of an unconfirmed contemporary account of Hekla 1947 tephra fall-out, a trace amount (<15 shards/cm^3) of light brown to brown cryptotephra shards (Fig. 4K–L) was detected in the uppermost peat, in Pervarvikonneva at 27 cm and in Kivihypönneva at 34 cm depth (sites 10 and 12 in Figs 1 and 5). At Kivihypönneva this tephra occurs ca. 15 cm above the Askja 1875 tephra. Unfortunately, the geochemical characterisation of the shards failed due to a lack of material, and correlations to source eruptions could thus not be established. Absence of the Hekla 1947 tephra from Finnish sites is a surprising result, as its fall-out in Finland has long been considered a classic example of the potential for a smaller scale eruption to form a tephra isochrone in the far-distal field. Given that this research resulted in the identification of cryptotephra deposits from four older eruptions, we can rule out the possibility that our cores would have been too short to record the Hekla 1947 fall-out or that the chosen methodology would have impeded detection of volcanic glass grains.

The absence of the Hekla 1947 tephra from our sites could be explained by a patchy fall-out or post-depositional horizontal movement of shards that were deposited on snow cover. It was not possible to verify a connection between precipitation and the Hekla 1947 tephra fall-out in this study, but inspection of precipitation maps with locations of eyewitness reports of tephra fall-out reveals that tephra fell mainly south of the zone of highest precipitation and also in areas that experienced no or minimal (< 1 mm/24 h) precipitation (Fig. 2A–C). The snow-depth map from 30 March 1947 reveals that snow was present almost throughout the fall-out zone (Fig. 2D). It has been suggested that reworking processes by meltwater and winds concentrate tephra shards in microtopographic hollows over the melting snowpack surface, rendering the layer patchy on a small scale (Bergman *et al.*, 2004). In the case of the Hekla 1947 tephra, this is also supported by observations of the visible fall-out in Finland commonly occurring in depressions in the snowpack (Salmi, 1948). Additionally, post-depositional horizontal movement of tephra shards over peat surface has been experimentally verified (Payne and Gehrels, 2010). On the other hand, we have carefully investigated nearly 50 surface cores from over 30 peatland and lake sites within the fall-out zone without

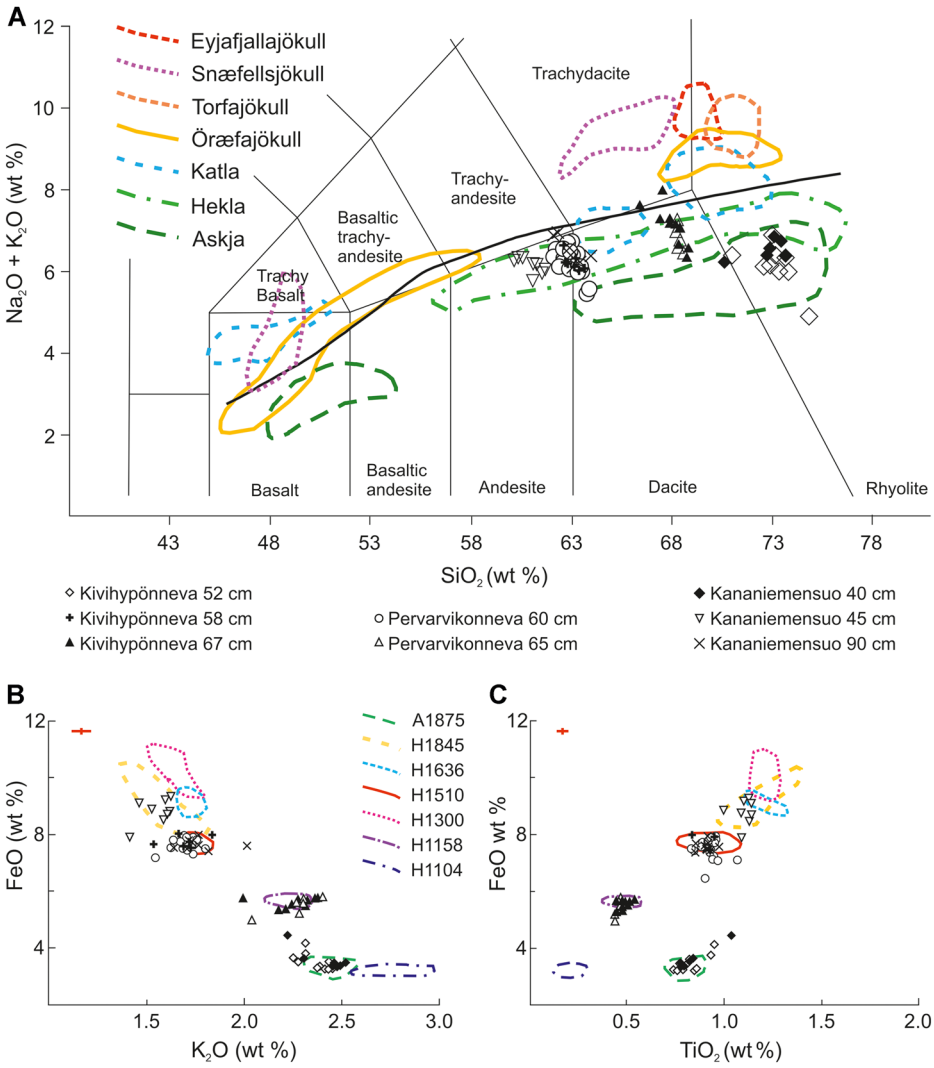

Figure 6. (A) Composition of Finnish cryptotephra deposits and geochemical envelopes of Icelandic volcanic systems shown on a total alkali–silica diagram. Nomenclature for volcanic rocks from Le Bas *et al.* (1986). High- and low-alkali products are separated by the Kuno line (Kuno, 1966) drawn in black. Data for the Icelandic volcanic systems are from Larsen *et al.*, 1999, and additionally from Sigvaldason, 1979; Prestvik, 1985; Steinthorsson *et al.*, 1985; Larsen *et al.*, 2001; Larsen *et al.*, 2002; Eiríksson *et al.*, 2004; Sverrisdóttir, 2007; Guðmundsdóttir *et al.*, 2011b; Óladóttir *et al.*, 2011; Kalliokoski *et al.*, 2019. (B–C) Comparison of FeO/K_2O and FeO/TiO_2 ratios of Finnish cryptotephra deposits and proximal deposits from selected historical Icelandic eruptions. The red error bar in the figure represents two standard deviations of repeated analysis of the secondary standards. Data are mainly from Larsen *et al.*, 1999. Additionally, for Hekla 1636 from Guðmundsdóttir *et al.*, 2016, for Hekla 1300 from Larsen *et al.*, 2002, and for Hekla 1845 from Watson *et al.*, 2015 and this study (Table S1). [Color figure can be viewed at wileyonlinelibrary.com]

finding the Hekla 1947 tephra. Even if post-depositional horizontal redistribution of cryptotephra could explain the lack of Hekla 1947 deposits in some of the coring sites, the same processes should have concentrated the tephra into others and at least some of the 50 cores would be expected to contain a detectable layer.

Preservation potential of volcanic glass in acidic environments

Poor post-depositional preservation of cryptotephra is another possible explanation for the absence of the Hekla 1947 tephra from Finnish sites. It has been suggested that geochemical alteration or even a total dissolution of small and vesicular volcanic glass shards, and basaltic glass specifically, takes place in acidic environments, such as peat bogs, or during acid digestion laboratory procedures (Pollard *et al.*, 2003; Blockley *et al.*, 2005). In Finland the environment is prone to acidification due to the prevailing base-poor and resistant granitic bedrock. Peat pH has been measured to range from 2.8–4.4 in raised peat bogs to 4.0–5.2 in fens (Martikainen *et al.*, 1993; Laine *et al.*, 1995; Jaatinen *et al.*, 2005). Considering this, poor preservation of andesitic–dacitic shards in an acidic bog environment might contribute to the apparent absence of the Hekla 1947 tephra in Finland. The degree of susceptibility of volcanic glass to geochemical alteration in acidic and basic conditions is still a matter of debate and two recently conducted experiments on the effects of strong acids and bases on volcanic glass particles during laboratory procedures give contradictory results (Monteath *et al.*, 2019; Cooper *et al.*, 2019a). The results of Monteath *et al.* (2019) do not support the idea of readily soluble volcanic glass, whereas Cooper *et al.* (2019a) found the geochemical alteration in andesitic and basaltic glass to be significant enough to result in possible miscorrelations when tracing the source eruptions of cryptotephra. According to Cooper *et al.* (2019a), a further implication of the observed alteration of low-silica glass would be its poorer stability in acidic peat bogs over longer timescales, which might partly explain the scarcity of basaltic glass in North European cryptotephra records (e.g. Wastegård and Davies 2009; Lawson *et al.*, 2012). However, in the case of the andesitic–dacitic Hekla 1947 tephra, its residence time in an acidic peat environment would be short; merely 67 years at the time of coring. A total dissolution of the shards is therefore considered unlikely, especially when the older andesitic Hekla 1845 and andesitic–dacitic Hekla 1510 tephras,

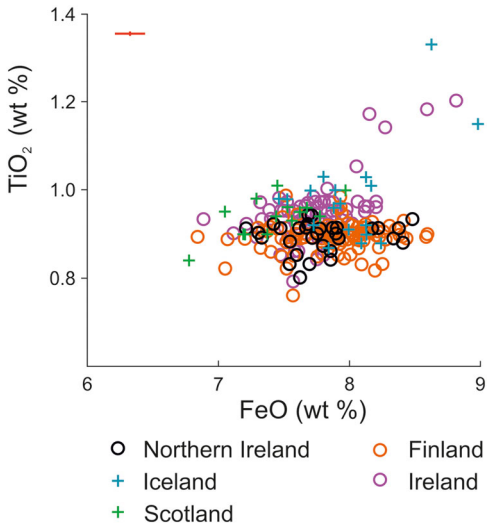

Figure 7. Comparison of TiO_2/FeO ratios of Hekla 1947 tephra in Finland, other distal sites and Iceland. The red error bar in the plot represents two standard deviations of repeated analysis of the secondary standards. Geochemical data from Larsen *et al.*, 1999; Housley *et al.*, 2010; Swindles *et al.*, 2010; Rea *et al.*, 2012; Watson *et al.*, 2015. [Color figure can be viewed at wileyonlinelibrary.com]

that have been calculated to have approximately the same theoretical stability as Hekla 1947 (Pollard *et al.*, 2003), are preserved at the Finnish sites. It is, however, possible that the preservation potential of tephra at any single site may vary through time due to changing environmental conditions. For example, it has been shown that air pollution inducing acidification of surface waters in Fennoscandia commenced in the 1940s and accelerated in the 1960s with increased combustion of fossil fuels (Tolonen and Jaakkola, 1983; Renberg, 1990). At that time, the Hekla 1947 tephra would still have resided at a shallow depth in the peat where acid rain likely resulted in elevated acidity, contributing to higher leaching rates of volcanic glass. The draining of peatlands has also contributed to the increased acidity of near-surface peat through lowering of the water table (Laine *et al.*, 1995; Jaatinen *et al.*, 2005). As the older tephra deposits, such as Hekla 1845 and 1510, lie deeper in the peat stratigraphy they would have been less affected by the acidification trend of the previous decades, which could explain their better preservation.

When the geochemical composition of the pristine Hekla 1947 shards in this study is compared with the composition of the Hekla 1947 cryptotephra layer in Northern Ireland (Rea *et al.*, 2012), no sign of geochemical alteration is detected in the Northern Irish shards that were retrieved from peat bogs and extracted using acid digestion. This is in line with the observations of Watson *et al.* (2015) who found no significant geochemical alteration in any of the rhyolitic Hekla 1104 or trachydacitic Sn-1 cryptotephra shards from lake (pH 7) or bog sites (pH 5.9) in Sweden. It could be argued that surface waters and peat bogs in Ireland and Britain would be generally less acidic than their Finnish and Swedish counterparts due to more base-rich bedrock, and thus favour the preservation of volcanic glass. However, atmospheric deposition of SO_2 emissions has driven acidification of surface waters in Ireland as well (Leira *et al.*, 2007) and peat pH of 3.5–8.5 has been measured in peatlands in Ireland and the UK (Wheeler and Proctor, 2000). Therefore, the acidic conditions of the Finnish peatlands alone do not sufficiently well explain the absence of the Hekla 1947 at Finnish sites. Whatever the reason(s) for the absence of Hekla 1947 tephra from the Finnish sites may be, our results imply that the chances of finding Hekla 1947 tephra in Finland are poor and it is unlikely to become an important isochrone in the region.

Dispersal patterns of Hekla 1158, Hekla 1510, Hekla 1845 and Hekla 1947 tephras

The Hekla 1158 eruption (VEI 4) began on 19 January and produced 0.2–0.6 km^3 of tephra (Janebo *et al.*, 2016). In Iceland, the dispersal axis of the 1158 tephra extends northeast from Hekla (Larsen *et al.*, 1999), and earlier identifications of this tephra in northern Norway (Pilcher *et al.*, 2005; Balascio *et al.*, 2011) and Sweden (Watson *et al.*, 2016; Cooper *et al.*, 2019b) as well as its absence from central and southern Sweden suggest that it reached Finland via a northerly transport route (Fig. 8). Hekla 1158 tephra was identified at just two peatland sites in this study. However, its dispersal area in Finland may well be wider than reported here, given that it was found in two of our three northernmost sites and no peatlands further north were investigated.

The Hekla 1845 eruption (VEI 4) started on 2 September and produced a minimum of 0.13 km^3 of tephra during its 1 h-long explosive opening phase (Guðnason *et al.*, 2018). In Iceland the axis of tephra fall extends east-southeast of Hekla (Guðnason *et al.*, 2018). Based on eyewitness reports from the Shetland Islands, Orkney and the Faroe Islands (Thorarinsson, 1981; Guðnason *et al.*, 2018) as well as earlier identification of this tephra in the Faroe Islands (Wastegård, 2002), Northern Ireland (Watson *et al.*, 2015) and Wales (Watson *et al.*, 2017), we postulate the transport pathway of this tephra to be similar to that of the Hekla 1947 tephra (Fig. 8). Dispersal of the Hekla 1845 tephra further east towards southern Finland along a curving pathway is also supported by observations of a volcanic haze in Sassnitz on the German coast of the Baltic Sea 4–5 days after the eruption (Fig. 8; Boll 1846 in Thorarinsson, 1981).

The Hekla 1510 eruption (VEI 4) began on 25 July and produced around 0.33 km^3 of tephra (Thorarinsson, 1967). Occurrence of the Hekla 1510 tephra has been reported to be patchy within its dispersal area in the UK (Dugmore *et al.*, 1995; Lawson *et al.*, 2012). In Finland, significantly further away from the source volcano, the occurrence of this tephra would be expected to be even more sporadic. Interestingly, our results indicate that Hekla 1510 tephra is quite widespread in Finland, and some of the unidentified deposits at our sites may well derive from the same eruption based on their stratigraphical position and the appearance of shards. For example, just one analysis was obtained from a cryptotephra deposit in Rehtsuo at 55 cm depth (Fig. 5), but the geochemical composition matches that of the Hekla 1510 tephra (Table S1).

The presence of Hekla 1845 and Hekla 1510 tephras in Ireland, the UK and Finland and their apparent absence from the rest of Fennoscandia and the European mainland indicates that their dispersal patterns are probably as complex as that of the Hekla 1947 tephra (Figs 1 and 8). However, using the absence of a cryptotephra to determine its dispersal in the distal area is not straightforward due to the many post-depositional processes and preservation issues that may impede cryptotephra detection (see Watson *et al.*, 2015 and references therein). This holds true especially for tephra originating from smaller scale eruptions, since tephra deposits consisting of scarce shards may be masked by the nearby presence of other more prominent layers. For example, cryptotephra originating from the Askja 1875 eruption (VEI 5) that produced 1.8 km^3 of tephra (Carey *et al.*, 2010), forms common deposits with high shard concentrations throughout Sweden, Norway and Finland (Wastegård, 2005; Davies *et al.*, 2007; Carey *et al.*, 2010; Kalliokoski *et al.*, 2019). If shard concentration profiles indicate the presence of a diffuse tephra layer and a sample for EPMA comprises only the depth of maximum shard concentration, tephra from smaller eruptions that are relatively close in age to the dominant eruption may be interpreted as a result of contamination or post-depositional

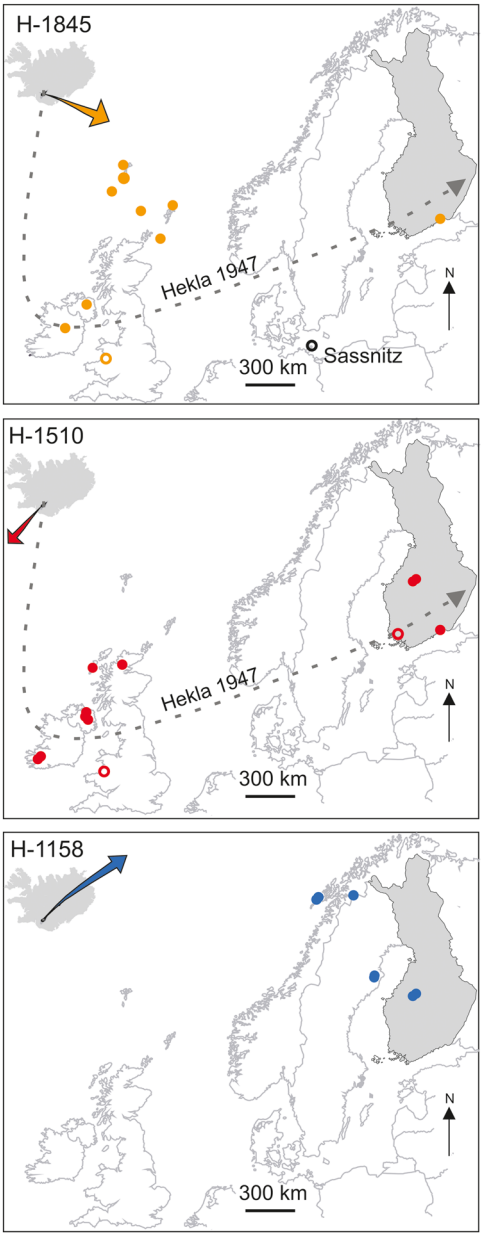

Figure 8. Maps showing the occurrence of Hekla 1845, Hekla 1510 and Hekla 1158 tephras in Northern Europe. Circles mark tentative correlations and dots geochemically confirmed cryptotephra deposits or contemporary eyewitness reports of fall-out. Axes of tephra fall within Iceland are from Larsen *et al.*, 1999 and Guðnason *et al.*, 2018. The arrow marking the main dispersal axis of Hekla 1947 tephra based on prevailing wind directions is from Salmi (1948). Data for sites of cryptotephra detection and eyewitness reports are from Dugmore *et al.*, 1995; Pilcher *et al.*, 1996; Wastegård, 2002; Pilcher *et al.*, 2005; Balascio *et al.*, 2011; Reilly and Mitchell, 2015; Watson *et al.*, 2015, 2016 and 2017; Guðnason *et al.*, 2018; Cooper *et al.*, 2019b. [Color figure can be viewed at wileyonlinelibrary.com]

reworking of the primary fall-out deposit and therefore remain unanalysed. As the technique of concentrating cryptotephra shards for EPMA by using a micromanipulator is relatively new, obtaining robust geochemical results from cryptotephra deposits with scarce shards has previously been very difficult and earlier research has focused mainly on the layers with the highest shard concentrations.

Significance for Finnish tephrochronology

The presence of four historical Icelandic cryptotephra layers in Finnish peat bogs indicates a great potential for using tephrochronology as a dating method in environmental research in the region. The most common cryptotephra layer in southern and middle Finland, the Askja 1875 tephra, was geochemically identified at six sites and was possibly present in two others. Hekla 1510 and Hekla 1158 tephras were found at three and two sites, respectively. However, their occurrence in Finland may be more common than reported here. Some of the detected cryptotephra horizons remain as yet unanalysed, and at more than half of the research sites only the uppermost 50 cm of peat were investigated, whereas the Hekla 1510 and Hekla 1158 cryptotephras were found deeper than 50 cm. In contrast, the Hekla 1845 cryptotephra was identified only in the southernmost site and, considering its occurrence depth just a couple of centimetres below the Askja 1875 horizon, it would probably have been detected had it been present at the other investigated sites. We suggest that at least the Askja 1875, Hekla 1510 and Hekla 1158 tephras may all become important marker layers in environmental research focusing on the past millennium, an era of increasing anthropogenic influence in Finland.

In this study, the Hekla 1845 and Hekla 1510 cryptotephras are identified for the first time outside of Ireland, the UK and the Faroes and their confirmed dispersal is extended significantly further east. The occurrence of Hekla 1845, Hekla 1510 and Hekla 1158 horizons in Finland is also an important implication for the potential of Icelandic eruptions of VEI ≤ 4 to create widely dispersed isochrones in the distal area, which allow inter-regional correlations to be made. Identification of four historical Icelandic tephras in Finland, as well as the fall-out of Hekla 1947 tephra (Salmi, 1948), the detection of the Eyjafjallajökull 2010 tephra in Finnish airspace (Davies *et al.*, 2010) and the identification of the Grímsvötn 2011 tephra in surface layer air in southern Finland (Kerminen *et al.*, 2011) highlight that volcanic ash from Icelandic eruptions is frequently carried to Finland. Furthermore, our results demonstrate that in addition to a direct eastward dispersal from Iceland, ash clouds may travel to Finland along both northerly and southerly transport routes. This implies that assuming a direct eastward transport route for Icelandic volcanic ash and estimating the frequency of volcanic ash events in Finnish airspace by extrapolating from the well-established Swedish and Norwegian tephrochronologies would give misleading results. This finding stresses the importance of further tephrochronological research in Finland and supports the predictions from simulations of volcanic ash transport of a high probability (46%) of tephra fall-out at Helsinki airport even after a moderate Hekla eruption (Leadbetter and Hort, 2011).

Conclusions

Hekla 1947 tephra was searched from 25 peatlands in southern and central Finland. Despite careful inspection of 47 surface peat cores and monoliths, no cryptotephra deposits could be attributed to the Hekla 1947 eruption. On the other hand, Hekla 1845, Hekla 1510 and Hekla 1158 cryptotephras were identified for the first time in Finland and their known dispersal areas were extended significantly eastwards. The presence of these tephras in Finland demonstrates that isochrones from Icelandic smaller scale eruptions are more extensive than previously realised. In addition, Askja 1875 cryptotephra was identified at two new sites in Finland. This result highlights the importance of Askja 1875 as the most prominent historical cryptotephra horizon in the region. Our results also reveal that in addition to a direct eastward dispersal route the ash clouds from Icelandic volcanic eruptions can be

transported to Finland along complex southerly and northerly dispersal routes. Absence of the Hekla 1947 tephra from its previously inferred fall-out zone in Finland remains unexplained and could be an indication of either post-depositional reworking of shards or poorer preservation potential of andesitic glass in peatlands during the 20th century due to increasingly acidic conditions caused by air pollution-induced acid rain and lowering of the water table. The identification of four historical Icelandic cryptotephras in Finnish peatlands demonstrates the potential of cryptotephra studies in Finland and is an important step towards building a Finnish tephrochronological framework.

Supporting information

Additional supporting information may be found in the online version of this article at the publisher's web-site.

Supporting Table S1. Electron microprobe analysis data for Hekla 1947 sample collection (Salmi 1948), proximal sample of Hekla 1845 tephra and cryptotephra horizons in Finnish peatlands.

Acknowledgements. We thank Sami Jokinen for assistance with field work in Finland and Dr Maria Janebo for field assistance in Iceland. Professor Siwan Davies and Dr Gwydion Jones at Swansea University are thanked for their help with micromanipulator work. We are grateful to Dr Chris Hayward for support with EPMA at the University of Edinburgh. Financial support for field work and EPMA was received from the Finnish Cultural Foundation, Varsinais-Suomi Regional Fund and Suomen Tiedeseura. Maarit Kalliokoski acknowledges funding from the Nordic Volcanological Centre at the University of Iceland and the Doctoral Programme in Biology, Geography and Geology at the University of Turku.

Data availability statement

The data that support the findings of this study are available in the supplementary material to this article.

References

Balascio NL, Wickler S, Narmo LE *et al*. 2011. Distal cryptotephra found in a Viking boathouse: the potential for tephrochronology in reconstructing the Iron Age in Norway. *Journal of Archaeological Science* **38**: 934–941.

Bergman J, Wastegård S, Hammarlund D *et al*. 2004. Holocene tephra horizons at Klocka Bog, west-central Sweden: aspects of reproducibility in subarctic peat deposits. *Journal of Quaternary Science* **19**: 241–249.

Blockley SPE, Pyne-O'Donnell SDF, Lowe JJ *et al*. 2005. A new and less destructive laboratory procedure for the physical separation of distal glass tephra shards from sediments. *Quaternary Science Reviews* **24**: 1952–1960.

Boygle J. 1999. Variability of tephra in lake and catchment sediments, Svínavatn, Iceland. *Global and Planetary Change* **21**: 129–149.

Boygle J. 2004. Towards a Holocene tephrochronology for Sweden: geochemistry and correlation with the North Atlantic tephra stratigraphy. *Journal of Quaternary Science* **19**: 103–109.

Bronk Ramsey C. 2009. Bayesian analysis of radiocarbon dates. *Radiocarbon* **51**: 337–360.

Carey RJ, Houghton BF, Thordarson T. 2010. Tephra dispersal and eruption dynamics of wet and dry phases of the 1875 eruption of Askja volcano, Iceland. *Bulletin of Volcanology* **72**: 259–278.

Cooper CL, Savov IP, Swindles GT. 2019a. Standard chemical-based tephra extraction methods significantly alter the geochemistry of volcanic glass shards. *Journal of Quaternary Science* **34**: 697–707.

Cooper CL, Swindles GT, Watson EJ. 2019b. Evaluating tephrochronology in the permafrost peatlands of northern Sweden. *Quaternary Geochronology* **50**: 16–28.

Davies SM, Abbott PM, Pearce NJG *et al*. 2012. Integrating the INTIMATE records using tephrochronology: rising to the challenge. *Quaternary Science Reviews* **36**: 11–27.

Davies SM, Elmquist M, Bergman J *et al*. 2007. Cryptotephra sedimentation processes within two lacustrine sequences from west central Sweden. *The Holocene* **17**: 319–330.

Davies SM, Larsen G, Wastegård S *et al*. 2010. Widespread dispersal of Icelandic tephra: how does the Eyjafjöll eruption of 2010 compare to past Icelandic events? *Journal of Quaternary Science* **25**: 605–611.

Dugmore AJ, Larsen G, Newton AJ. 1995. Seven tephra isochrones in Scotland. *The Holocene* **5**: 257–266.

Dugmore AJ, Newton AJ, Edwards KJ *et al*. 1996. Long-distance marker horizons from small-scale eruptions: British tephra deposits from the AD 1510 eruption of Hekla, Iceland. *Journal of Quaternary Science* **11**: 511–516.

Eiríksson J, Larsen G, Knudsen KL *et al*. 2004. Marine reservoir age variability and water mass distribution in the Iceland Sea. *Quaternary Science Reviews* **23**: 2247–2268.

Gehrels MJ, Newnham RM, Lowe DJ *et al*. 2008. Towards rapid assay of cryptotephra in peat cores: Review and evaluation of various methods. *Quaternary International* **178**: 68–84.

Guðmundsdóttir ER, Larsen G, Eiríksson J. 2011a. Two new Icelandic tephra markers: the Hekla Ö tephra layer, ~6060 cal. yr BP, and Hekla DH tephra layer, ~6650 cal. yr. BP. Land-sea correlation of mid-Holocene tephra markers. *The Holocene* **21**: 629–639.

Guðmundsdóttir ER, Eiríksson J, Larsen G. 2011b. Identification and definition of primary and reworked tephra in Late Glacial and Holocene marine shelf sediments off North Iceland. *Journal of Quaternary Science* **26**: 589–602.

Guðmundsdóttir ER, Larsen G, Björck S *et al*. 2016. A new high-resolution Holocene tephra stratigraphy in eastern Iceland: Improving the Icelandic and North Atlantic tephrochronology. *Quaternary Science Reviews* **150**: 234–249.

Guðnason J, Thordarson T, Houghton BF *et al*. 2018. The 1845 Hekla eruption: Grain-size characteristics of a tephra layer. *Journal of Volcanology and Geothermal Research* **350**: 33–46.

Hall VA. 1998. Recent landscape change and landscape restoration in Northern Ireland: a tephra-dated pollen study. Review of palaeobotany and palynology. *Review of Palaeobotany and Palynology* **103**: 59–68.

Hayward C. 2012. High spatial resolution electron probe microanalysis of tephras and melt inclusions without beam-induced chemical modification. *The Holocene* **22**: 119–25.

Housley RA, Blockley SPE, Matthews IP *et al*. 2010. Late Holocene vegetation and palaeoenvironmental history of the Dunadd area, Argyll, Scotland: chronology of events. *Journal of Archaeological Science* **37**: 577–593.

Jaatinen K, Tuittila ES, Laine J *et al*. 2005. Methane-oxidizing bacteria in Finnish raised mire complex: effects of site fertility and drainage. *Microbial Ecology* **50**: 429–439.

Janebo MH, Thordarson T, Houghton BF *et al*. 2016. Dispersal of key subplinian–Plinian tephras from Hekla volcano, Iceland: implications for eruption source parameters. *Bulletin of Volcanology* **78**: 66.

Jensen BJL, Pyne-O'Donnell S, Plunkett G *et al*. 2014. Transatlantic distribution of the Alaskan White River Ash. *Geology* **42**: 875–878.

Jones G, Davies SM, Staff RA *et al*. 2019. Traces of volcanic ash from the Mediterranean, Iceland and North America in a Holocene record from south Wales, UK. *Journal of Quaternary Science* **35**: 163–174.

Jones G, Lane CS, Brauer A *et al*. 2018. The Lateglacial to early Holocene tephrochronological record from Lake Hämelsee, Germany: a key site within the European tephra framework. *Boreas* **47**: 28–40.

Jónsson DF, Guðmundsdóttir ER, Larsen G *et al*. 2020. The multi-component Hekla Ö Tephra, Iceland: a complex widespread mid-Holocene tephra layer. *Journal of Quaternary Science* **35**: 410–421.

Kalliokoski M, Wastegård S, Saarinen T. 2019. Rhyolitic and dacitic component of the Askja 1875 tephra in southern and central Finland: first step towards a Finnish tephrochronology. *Journal of Quaternary Science* **34**: 29–39.

Kerminen V-M, Niemi JV, Timonen H *et al*. 2011. Characterisation of a volcanic ash episode in southern Finland caused by the Grimsvötn eruption in Iceland in May 2011. *Atmospheric Chemistry and Physics* **11**: 12227–12239.

Kuno H. 1966. Lateral variation of basalt magma type across continental margins and island arcs. *Bulletin Volcanologique* **29**: 195–222.

Laine J, Vasander H, Laiho R. 1995. Long-term effects of water level drawdown on the vegetation of drained pine mires in southern Finland. *Journal of Applied Ecology* **32**: 785–802.

Lane CS, Cullen VL, White D *et al*. 2014. Cryptotephra as a dating and correlation tool in archaeology. *Journal of Archaeological Science* **42**: 42–50.

Langdon PG, Barber KE. 2004. Snapshots in time: precise correlations of peat-based proxy climate records in Scotland using mid-Holocene tephras. *The Holocene* **14**: 21–33.

Larsen G, Dugmore A, Newton A. 1999. Geochemistry of historical-age silicic tephras in Iceland. *The Holocene* **9**: 463–471.

Larsen G, Eiríksson J, Knudsen KL *et al*. 2002. Correlation of late Holocene terrestrial and marine tephra markers, north Iceland: implications for reservoir age changes. *Polar Research* **21**: 283–290.

Larsen G, Newton AJ, Dugmore AJ *et al*. 2001. Geochemistry, dispersal, volumes and chronology of Holocene silicic tephra layers from the Katla volcanic system, Iceland. *Journal of Quaternary Science* **16**: 119–132.

Larsen G, Róbertsdóttir BG, Óladóttir BA *et al*. 2020. A shift in eruption mode of Hekla volcano, Iceland, 3000 years ago: two-coloured Hekla tephra series, characteristics, dispersal and age. *Journal of Quaternary Science* **35**: 143–154.

Larsen G, Thorarinsson S. 1977. H4 and other acid Hekla tephra layers. *Jökull* **27**: 28–46.

Larsen JJ, Noe-Nygaard N. 2013. Lateglacial and early Holocene tephrostratigraphy and sedimentology of the Store Slotseng basin, SW Denmark: a multi-proxy study. *Boreas* **43**: 349–361.

Lawson IT, Swindles GT, Plunkett G *et al*. 2012. The spatial distribution of Holocene cryptotephras in north-west Europe since 7 ka: implications for understanding ash fall events from Icelandic eruptions. *Quaternary Science Reviews* **41**: 57–66.

Leadbetter SJ, Hort MC. 2011. Volcanic ash hazard climatology for an eruption of Hekla volcano, Iceland. *Journal of Volcanology and Geothermal Research* **199**: 230–241.

Le Bas MJ, Maitre RWL, Streckeisen A *et al*. 1986. A chemical classification of volcanic rocks based on the total alkali-silica diagram. *Journal of Petrology* **27**: 745–750.

Leira M, Cole EE, Mitchell FJG. 2007. Peat erosion and atmospheric deposition impacts on an oligotrophic lake in eastern Ireland. *Journal of Paleolimnology* **38**: 49–71.

MacLeod A, Brunnberg L, Wastegård S *et al*. 2014. Lateglacial cryptotephra detected within clay varves in Östergötland, south-east Sweden. *Journal of Quaternary Science* **29**: 605–609.

Martikainen PJ, Nykänen H, Crill P *et al*. 1993. Effect of a lowered water table on nitrous oxide fluxes from northern peatlands. *Nature* **366**: 51–53.

Monteath AJ, Teuten AE, Hughes PDM *et al*. 2019. Effects of the peat acid digestion protocol on geochemically and morphologically diverse tephra deposits. *Journal of Quaternary Science* **34**: 269–274.

Newhall CG, Self S. 1982. The Volcanic Explosivity Index (VEI): an estimate of explosive magnitude for historical volcanism. *Journal of Geophysical Research* **87**: 1231–1238.

Óladóttir BA, Larsen G, Sigmarsson O. 2011. Holocene volcanic activity at Grímsvötn, Bárðarbunga and Kverkfjöll subglacial centres beneath Vatnajökull, Iceland. *Bulletin of Volcanology* **73**: 1187–1208.

Payne R, Gehrels M. 2010. The formation of tephra layers in peatlands: an experimental approach. *Catena* **81**: 12–23.

Persson C. 1966. Försök till tefrokronologisk datering av några svenska torvmossar. *Geologiska föreningen i Stockholm Förhandlingar* **88**: 361–394.

Pilcher J, Bradley RS, Francus P *et al*. 2005. A Holocene tephra record from the Lofoten Islands, Arctic Norway. *Boreas* **34**: 136–156.

Pilcher JR, Hall VA. 1992. Towards a tephrochronology for the Holocene of the north of Ireland. *The Holocene* **2**: 255–259.

Pilcher JR, Hall VA, McCormac FG. 1996. An outline tephrochronology for the Holocene of the north of Ireland. *Journal of Quaternary Science* **11**: 485–494.

Plunkett G, Pilcher JR. 2018. Defining the potential source region of volcanic ash in northwest Europe during the Mid- to Late Holocene. *Earth-Science Reviews* **179**: 20–37.

Pollard AM, Blockley SPE, Ward KR. 2003. Chemical alteration of tephra in the depositional environment: theoretical stability modelling. *Journal of Quaternary Science* **18**: 385–394.

Prestvik T. 1985. *Petrology of Quaternary volcanic rocks from Öræfi, southeast Iceland. Report 21*. Geologisk Institutt, Norges Tekniske Hojskole: Trondheim.

Rea HA, Swindles GT, Roe HM. 2012. The Hekla 1947 tephra in the north of Ireland: regional distribution, concentration and geochemistry. *Journal of Quaternary Science* **27**: 425–431.

Reilly E, Mitchell FJG. 2015. Establishing chronologies for woodland small hollow and mor humus deposits using tephrochronology and radiocarbon dating. *The Holocene* **25**: 241–252.

Reimer PJ, Bard E, Bayliss A *et al*. 2013. IntCal13 and Marine13 radiocarbon age calibration curves 0–50,000 years cal BP. *Radiocarbon* **55**: 1869–1887.

Renberg I. 1990. A 12 600 year perspective of the acidification of Lilla Öresjön, southwest Sweden. *Philosophical Transactions of the Royal Society of London. Series B, Biological Sciences* **327**: 357–361.

Salmi M. 1948. The Hekla ashfalls in Finland. AD 1947. *Comptes Rendus de la Société Geologique de Finlande* **21**: 81–96.

Sigvaldason GE. 1974. The petrology of Hekla and origin of silicic rocks in Iceland, *The eruption of Hekla 1947-48. Societas Scientarium Islandica; Reykjavík* 1–44.

Sigvaldason GE. 1979. *Rifting, magmatic activity and interaction between acid and silicic liquids. The Askja 1875 eruption in Iceland*. Report 7903. Nordic Volcanological Institute, University of Iceland: Reykjavík, Iceland.

Steinthorsson S, Oskarsson N, Sigvaldason GE. 1985. Origin of alkali basalts in Iceland: a plate tectonic model. *Journal of Geophysical Research* **90**: 10027–10042.

Sverrisdóttir G. 2007. Hybrid magma generation preceding Plinian silicic eruptions at Hekla, Iceland: evidence from mineralogy and chemistry of two zoned deposits. *Geological Magazine* **144**: 643–659.

Swindles GT, Blundell A, Roe HM *et al*. 2010. A 4500-year proxy climate record from peatlands in the North of Ireland: the identification of widespread summer 'drought phases'? *Quaternary Science Reviews* **29**: 13–14.

Thorarinsson S. 1954. The tephra fall from Hekla on March 29 1947. In *The eruption of Hekla 1947–1948 I*, Einarsson T, Kjartansson G, Thorarinsson S (eds). Societas Scientiarum Islandica: Reykjavík; 1–68.

Thorarinsson S. 1967. The eruptions of Hekla in historical times. A tephrochronological study. In *The eruption of Hekla 1947–1948 II*, Einarsson T, Kjartansson G, Thorarinsson S (eds). Societas Scientiarum Islandica: Reykjavík; 1–170.

Thorarinsson S. 1981. Greetings from Iceland. Ash-falls and volcanic aerosols in Scandinavia. *Geografiska Annaler* **63**: 109–118.

Thorsteinsdóttir ES, Guðmundsdóttir ER, Larsen G. 2015. Grain characteristics of tephra from the sub-glacial SILK-LN Katla eruption ~3400 years ago and the sub-aerial Hekla eruption in 1947. *Jökull* **65**: 29–49.

Timms RGO, Matthews IP, Lowe JJ *et al*. 2019. Establishing tephrostratigraphic frameworks to aid the study of abrupt climatic and glacial transitions: a case study of the Last Glacial-Interglacial Transition in the British Isles (c. 16-8 ka BP). *Earth-Science Reviews* **192**: 34–64.

Tolonen K, Jaakkola T. 1983. History of lake acidification and air pollution studied on sediments in South Finland. *Annales Botanici Fennici* **20**: 57–78.

Turney CSM. 1998. Extraction of rhyolitic component of Vedde microtephra from minerogenic lake sediments. *Journal of Paleolimnology* **19**: 199–206.

Vakhrameeva P, Portnyagin M, Ponomareva V *et al*. 2020. Identification of Icelandic tephras from the last two millennia in the White Sea region (Vodoprovodnoe peat bog, northwestern Russia). *Journal of Quaternary Science* **35**: 493–504.

van der Bilt WGM, Lane CS, Bakke J. 2017. Ultra-distal Kamchatkan ash on Arctic Svalbard: towards hemispheric cryptotephra correlation. *Quaternary Science Reviews* **164**: 230–235.

van der Bilt WGM, Lane CS. 2019. Lake sediments with Azorean tephra reveal ice-free conditions on coastal northwest Spitsbergen during the Last Glacial Maximum. *Science Advances* **5**: eaaw5980.

Wastegård S. 2002. Early to middle Holocene silicic tephra horizons from the Katla volcanic system, Iceland: new results from the Faroe Islands. *Journal of Quaternary Science* **17**: 723–730.

Wastegård S. 2005. Late Quaternary tephrochronology of Sweden: a review. *Quaternary International* **130**: 49–62.

Wastegård S, Davies SM. 2009. An overview of distal tephrochronology in northern Europe during the last 1000 years. *Journal of Quaternary Science* **24**: 500–512.

Wastegård S, Rundgren M, Schoning K *et al*. 2008. Age, geochemistry and distribution of the mid-Holocene Hekla-S/Kebister tephra. *The Holocene* **18**: 539–549.

Watson EJ, Swindles GT, Lawson IT *et al*. 2015. Spatial variability of tephra and carbon accumulation in a Holocene peatland. *Quaternary Science Reviews* **124**: 248–264.

Watson EJ, Swindles GT, Lawson IT *et al*. 2016. Do peatlands or lakes provide the most comprehensive distal tephra records? *Quaternary Science Reviews* **139**: 110–128.

Watson EJ, Swindles GT, Lawson IT *et al*. 2017. The presence of Holocene cryptotephra in Wales and southern England. *Journal of Quaternary Science* **32**: 493–500.

Wheeler BD, Proctor MCF. 2000. Ecological gradients, subdivisions and terminology of north-west European mires. *Journal of Ecology* **88**: 187–203.

